Orbital magnetization of a Mott insulator, V_2O_3, revealed by resonant x-ray Bragg diffraction

S. W. Lovesey, K. S. Knight, and D. S. Sivia
ISIS Facility, Rutherford Appleton Laboratory, Oxfordshire OX11 0QX, United Kingdom
(Received 14 March 2002; published 16 May 2002)

Structure factors calculated for x-ray Bragg diffraction by magnetically ordered vanadium sesquioxide, V_2O_3, with signal enhancement from the vanadium *K*-shell resonance, are compared with data gathered in azimuthal-angle scans at space-group forbidden reflections. Diffraction enhanced by a *K*-shell resonance reveals properties of the orbital magnetization in the valence shell of the resonant ion, whereas other core states, which have two partners because of the spin-orbit interaction, reveal properties of both the spin and orbital magnetization in the valence shell. Agreement on all issues between observed and calculated Bragg intensities support the use of an atomic model for the interpretation of data. The reflections are shown to be purely magnetic, and associated with the orbital magnetic moment and the octupole moment of a vanadium ion. Reflections with a Miller index *h* even are analyzed to give the canting angle of the magnetic easy axis. Data from the rotated ($\pi'\sigma$) and unrotated ($\sigma'\sigma$) channels of scattering provide an angle consistent with an earlier interpretation of magnetic neutron diffraction. With *h* odd, diffraction enhanced by an $E1$ event is forbidden. Intensities enhanced by an $E2$ event are from anisotropic components of the octupole moment. Analysis of azimuthal-angle scans, with *h* even and *h* odd, provides estimates of orbital moments that in the future can be confronted with *ab initio* calculations of the electronic properties of V_2O_3. By and large, the complicated pattern of azimuthal-angle scans can be attributed to the low symmetry (monoclinic) structure adopted below the Néel temperatures.

DOI: 10.1103/PhysRevB.65.224402 PACS number(s): 71.30.+h, 75.50.Ee, 78.70.Ck

I. INTRODUCTION

Vanadium sesquioxide (V_2O_3) displays a number of electronic, magnetic, and structural properties that are challenging to interpret and explain.[1–7] At room temperature V_2O_3 has the corundum structure with space group $R\bar{3}c$, and it is metallic and paramagnetic. (It is unique among the isostructural sesquioxides with respect to its small a/c ratio and metallic conductivity.) On reducing the temperature the corundum structure distorts to a monoclinic structure with space group $I2/a$. The structural transition in the temperature range 150–160 K is strongly first-order and ferroelastic. Accompanying the transition are a change from metallic to insulating behavior and the onset of antiferromagnetic order.[3] The metal-insulator transition is viewed as a classic Mott transition.

Recently, results from resonant x-ray Bragg diffraction experiments[8–10] have added to the wealth of knowledge about V_2O_3. We put forward an explanation of some key aspects of the observed x-ray diffraction pattern[11] in which the intensity is enhanced by the resonance at the *K* edge of a vanadium ion. Here we give a more complete account of the model employed and the work involved in calculating structure factors for resonance enhanced Bragg diffraction. Calculations for azimuthal-angle scans are also reported, and they are shown to provide a fully quantitative explanation of available data.[8–10] The success of our model in explaining the resonant x-ray-diffraction data distinguishes it from previous discussions[6] and permits us to draw specific conclusions about the orbital magnetization present in V_2O_3.

The data of interest have been gathered for Bragg reflections that are forbidden by the space group, and often called charge-forbidden reflections. In general, such reflections are due to spatial anisotropy in the charge distribution or a long-range magnetic order that is not indexed on the chemical structure. When long-range magnetic order is absent, the diffraction at charge-forbidden reflections is usually referred to as Templeton-Templeton scattering.[12,13] Intensities measured for different settings of the crystal rotated about the Bragg wave vector can provide direct information on the nature of the anisotropy and spatial symmetry. Tuning the primary x-ray energy to an inner-shell absorption edge makes the diffraction signal specific to the resonant ion, and for the case in hand this is a vanadium ion. Should the Bragg wave vector coincide with an axis of rotation through the site occupied by the resonant ion the azimuthal angle (ψ) meshes with the rotational periodicity, and the Bragg intensity displays a periodicity in ψ equal to twice the degree of the axis of rotation.[14,15] Such a configuration can be achieved in diffraction from the corundum structure,[11,14] and the observed azimuthal-angle scan is sixfold periodic. Broadly speaking, complexity in azimuthal-angle scans observed for magnetically ordered V_2O_3 (Refs. 8–10) is due to the low spatial symmetry of the monoclinic structure adopted by the crystal. While properties of a resonant vanadium ion carry a heavy imprint of a threefold axis of rotation, that controls properties in the corundum structure,[11] monoclinic Bragg wave vectors do not coincide with the trigonal axis of the corundum structure and it is this mismatch, between the wave vectors and the axis of rotation, that is largely responsible for the seemingly complex pattern of the azimuthal-angle scans. However, we can demonstrate that the scans do contain some very specific information on the orbital magnetization of V_2O_3.

The resonance-enhanced intensity is related to properties of the valence shell that accommodates the photoejected core electron in the intermediate state of the elastic scattering pro-

cess. Absorption at the K edge and an electric-dipole event $(E1)$ gives access to valence states with atomic p-like character, and an electric quadrupole event $(E2)$ at the same edge gives access to d-like states $(1s \rightarrow 3d)$. In terms of a pure $E2$ event we analyze diffraction data collected with the primary energy tuned to a feature in the pre-edge (5.464 keV and $\lambda = 2.27$ Å) of the vanadium K shell. The associated Bragg intensity is therefore attributed directly to properties of the $3d$ shell of a vanadium ion. As a function of the primary energy, the observed intensity is adequately described by a single oscillator. A $1s$ core state is not split by spin-orbit coupling and, in this instance, we can confidently ascribe the intensity to orbital moments[16] and spin moments are not-explicitly contributing. (Two studies of diffraction by NiO with enhancement from an $E2$ event at the K edge of the Ni ion[17] corroborate the absence of a contribution to scattering by spin magnetic moments.) For magnetically ordered V_2O_3 we have demonstrated that charge-forbidden reflections are due exclusively to the orbital magnetization[11] (specifically, the amplitude is the mean value of spherical tensors of odd rank that are odd with respect to time reversal). The intensity of such reflections must decrease on warming the sample and vanish with the loss of magnetic long-range order.

The existence in V_2O_3 of a large orbital magnetic moment (in the range of 35–40 % of the spin moment[3,8]), and pronounced magnetic anisotropy,[3] are signs of very effective spin-orbit coupling in the valence shell that forces orbitals to follow spin. From this stance orbital ordering is not viable, and models without the spin-orbit coupling cannot reproduce the magnetic properties of V_2O_3 (Refs. 6 and 7) revealed in the resonant x-ray-diffraction experiments under discussion. In the subsequent development V_2O_3 is described on the basis of experimentally determined chemical[2] and magnetic[3] structures with no added degrees of freedom.

Information on the crystal structure, which is based on observations reported by Dernier and Marezio,[2] is gathered in Sec. II together with the configuration of magnetic moments,[3] The second ingredient in the calculated structure factors is a model of resonance-enhanced Bragg diffraction. We employ an atomic model which should be adequate for a one-component intensity profile like the ones observed with V_2O_3 at the vanadium K-shell pre-edge.[8,9] After adopting a single oscillator to describe the intensity profile, the amplitude attached to the oscillator can be calculated without further approximation.[16] The atomic model for the event $1s \rightarrow 3d$, which is of interest to us here, shows that the amplitude is constructed from spherical tensors that describe the orbital properties of the $3d$ shell. After putting together the two ingredients it only remains to describe the geometry of the experiment, namely, the orientation of the crystal (a function of the azimuthal angle) in the frame of reference used for the polarizations and wave vectors of the primary and diffracted beams of x rays. These aspects of the calculation of the structure factors for unrotated $(\sigma'\sigma)$ and rotated $(\pi'\sigma)$ channels of scattering are described in Secs. III and IV. Thereafter, in Sec. V, we confront the structure factors with experimental data and, in section VI, draw conclusions about resonant x-ray Bragg diffraction by vanadium sesquioxide.

TABLE I. Components entering the structure factor of V_2O_3 in the monoclinic structure. The eight vanadium ions are labeled according to the scheme shown in Fig. 1, and $h+k+l$ is an odd integer. The angles appearing in the spatial phase factors are $\nu = 2\pi(xh+yk+zl)$ and $\varepsilon = 4\pi yk$, and values for (x, y, z) are mentioned in section 2.

Site label	Spatial phase factor	Atomic tensor
(1)	$e^{i\nu}$	$\langle T_Q^{(K)}(1)\rangle$
(2)	$-e^{i\nu}$	$(-1)^K\langle T_Q^{(K)}(1)\rangle$
(3)	$e^{i(\varepsilon-\nu+\pi h)}$	$\langle T_Q^{(K)}(3)\rangle$
(4)	$-e^{i(\varepsilon-\nu+\pi h)}$	$(-1)^K\langle T_Q^{(K)}(3)\rangle$
(5)	$e^{-i\nu}$	$\langle T_Q^{(K)}(5)\rangle$
(6)	$-e^{-i\nu}$	$(-1)^K\langle T_Q^{(K)}(5)\rangle$
(7)	$e^{i(\nu+\pi h-\varepsilon)}$	$\langle T_Q^{(K)}(7)\rangle$
(8)	$-e^{i(\nu+\pi h-\varepsilon)}$	$(-1)^K\langle T_Q^{(K)}(7)\rangle$.

II. CHEMICAL AND MAGNETIC STRUCTURES

At room temperature vanadium sesquioxide has a trigonal (corundum) structure with space group 167 $(R\bar{3}c)$. Lowering the temperature of the material induces distortions which include tilting of the trigonal (hexagonal-c) axis and a reduction of the point-group symmetry of sites occupied by vanadium ions from $3(C_3)$ to that of no symmetry.

The space group of the low-temperature monoclinic structure is number $15(I2/a)$, in which vanadium ions occupy sites 8 (f). This is a body-centered cell, and Bragg wave vectors $\tau_m(hkl)$ for charge reflections have the necessary condition $h+k+l$ an even integer. (Miller indices h, k, and l are integers.) In the published[3] neutron-diffraction patterns, magnetic reflections are indexed by $h+k+l$ odd, and Table I contains the corresponding spatial phase factors for the Bragg structure factor. The antiferromagnetic configuration of vanadium magnetic moments, displayed in Fig. 1, consists of sheets of moments with ferromagnetic alignment within $(010)_m$ layers, or hexagonal (110) layers, and moment reversal between adjacent layers. The moments are orientated along some easy axis in these layers, and we take ϕ as the canting angle with respect to the trigonal axis.

The trigonal basis vectors are $\mathbf{a}_h = a(1,0,0)$, $\mathbf{b}_h = a(-1/2,\sqrt{3}/2,0)$, and $\mathbf{c}_h = c(0,0,1)$ and the volume of the unit cell $= a^2c\sqrt{3}/2$. Following Dernier and Marezio,[2] in the use of an I-centered cell, from these vectors we generate monoclinic basis vectors $\mathbf{a}_m = [0,(1/\sqrt{3})2a,1/3c]$, $\mathbf{b}_m = \mathbf{a}_h$, and $\mathbf{c}_m = [0,(1/\sqrt{3})a,-1/3c]$, and the volume of the cell $= a^2c/\sqrt{3}$. The corresponding Bragg wave vector $\tau_m(hkl) \equiv (hkl)_m$ is

$$\boldsymbol{\tau}_m(hkl) = \frac{1}{a}\left[k,(1/\sqrt{3})(h+l),\frac{a}{c}(h-2l)\right]. \qquad (2.1)$$

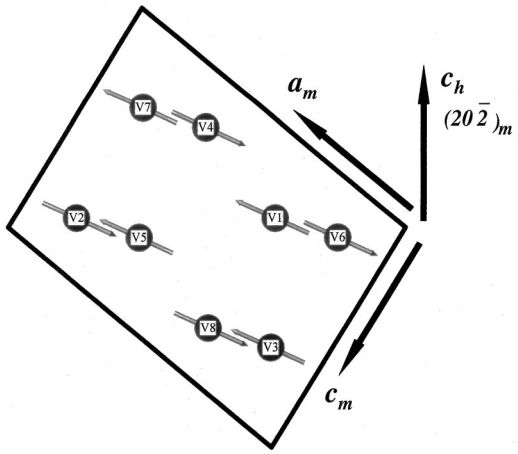

FIG. 1. Positions of the eight vanadium ions in the monoclinic unit cell together with the configuration of their magnetic moments which lie in the $\mathbf{a}_m-\mathbf{c}_m$ plane of the diagram. The monoclinic Bragg wave vector $(20\bar{2})_m$ is parallel to the trigonal axis $\mathbf{c}_h$, and $\mathbf{b}_m$ is normal to the plane of the diagram and parallel to $\mathbf{a}_h$.

We note that $(l0\bar{l})_m$ is parallel to $\mathbf{c}_h$ and $(2lkl)_m$ is normal to $\mathbf{c}_h$.

Referring to Fig. 1, the position coordinates of vanadium ions labeled (1) and (5) are (x, y, z) and $(-x,-y,-z)$, respectively, with $x=0.3438$, $y=0.0008$, and $z=0.2993$.[2,9] The positions of pairs (2) and (6) are related by a body-center translation to pairs (1) and (5). The position coordinates of (3) and (7) are $(\frac{1}{2}-x,y,-z)$ and $(\frac{1}{2}+x,-y,z)$, respectively, and the pairs (4) and (8), and (3) and (7) are related by the body-center translation. The body-center translation $(\frac{1}{2},\frac{1}{2},\frac{1}{2})_m=(a/2)(1,\sqrt{3},0)$ and $(\frac{1}{2},\frac{1}{2},\frac{1}{2})_m\tau_m(hkl)=\frac{1}{2}(h+k+l)$. Spatial phase factors listed in Table I are correct for $h+k+l$ which is an odd integer, and this condition on Miller indices provides a minus sign in factors for even relative to odd numbered sites. In writing out spatial phase factors in the structure factor it is convenient to define two angles, $\nu=2\pi(x,y,z)_m\tau_m(hkl)=2\pi(xh+yk+zl)$ and $\varepsilon=4\pi yk$.

III. STRUCTURE FACTOR FOR BRAGG DIFFRACTION BY MAGNETICALLY ORDERED V_2O_3

As a function of the energy of the primary x rays, the observed intensity of diffraction from V_2O_3 which is enhanced by electric-quadrupole $(E2)$ resonance has a simple shape[8,9] which is adequately described by a single oscillator. In this instance, the integrated intensity can be calculated without approximation,[16] and for a pure $E2$ absorption event $1s\rightarrow 3d$ the intensity is found to be proportional to the orbital moments of the $3d$ valence shell.[16,17] Here orbital moments are represented by atomic tensors $\langle\mathbf{T}^{(K)}\rangle$ of rank $K=0$, 1, 2, 3, and 4. (For electric-dipole absorption, the maximum K is 2.) In the structure factor, which is a scalar quantity, the atomic tensors appear in a scalar product with a tensor, denoted by $\mathbf{H}^{(K)}$, that describes the conditions of the primary and diffracted beams of x rays. It is convenient in the ensuing calculation to consider the quantity

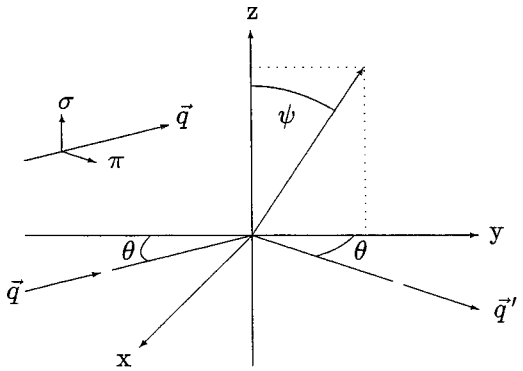

FIG. 2. The orthogonal states of polarization in the primary beam of x rays with σ polarization normal to the plane of scattering defined by the primary $(\mathbf{q})$ and diffracted $(\mathbf{q}')$ wave vectors. X rays are deflected through an angle 2θ and $\tau_m=\mathbf{q}-\mathbf{q}'$. Orthogonal axes (x, y, z) are related to the geometry of the experiment; the **x** axis is parallel to $-\tau_m$ and the **z** axis is normal to the plane of scattering and parallel to the σ polarization. An azimuthal-angle scan is rotation of the crystal by ψ about τ_m, and the origin $\psi=0$ is defined by a specified plane normal to the plane of scattering.

$$\Psi_Q^{(K)}=\sum_d \langle T_Q^{(K)}(\mathbf{d})\rangle\exp(i\boldsymbol{\tau}\cdot\mathbf{d}), \tag{3.1}$$

where $-K\leqslant Q\leqslant K$, $\mathbf{d}$ defines the position of a resonant vanadium ion in the unit cell, and τ is the Bragg wave vector for the reflection in question. With this notation the structure factor is[16,18]

$$F(\boldsymbol{\tau})=\sum_K (2K+1)^{1/2}\mathbf{H}^{(K)}\cdot\boldsymbol{\Psi}^{(K)}$$

$$=\sum_{K,Q}(2K+1)^{1/2}(-1)^Q H_{-Q}^{(K)}\Psi_Q^{(K)}. \tag{3.2}$$

The components $H_Q^{(K)}$ for unrotated $(\sigma'\sigma)$ and rotated $(\pi'\sigma)$ radiation are tabulated.[18] The tensor $\mathbf{H}^{(K)}$ and $\Psi^{(K)}$ are evaluated in the coordinate system that defines the experimental geometry. Referring to Fig. 2, σ polarization is perpendicular to the plane of scattering and parallel to the z-axis, and $\hat{\mathbf{q}}-\hat{\mathbf{q}}'=-2\sin\theta\hat{\mathbf{x}}$ and $\hat{\mathbf{q}}+\hat{\mathbf{q}}'=2\cos\theta\hat{\mathbf{y}}$, where θ is the Bragg angle.

We find it convenient initially to consider $\Psi_Q^{(K)}$ with respect to a second set of orthogonal axes (x,y,z) that include $\mathbf{a}_h=(a,0,0)=\mathbf{b}_m$ and $\mathbf{c}_h=(0,0,c)$. Thereafter we apply to $\Psi_Q^{(K)}$ rotations that describe the orientation of the crystal in the coordinates of the experimental geometry that apply to $\mathbf{H}^{(K)}$.

The spatial phase factors in $\Psi_Q^{(K)}$ are listed in Table I, and the eight resonant vanadium ions are labeled according to the scheme shown in Fig. 1. Following the discussion in Sec. II, the chemical environments of ions in the pairs (1) and (2), (5) and (6), (7) and (8), and (3) and (4) are taken to be identical. Moreover, the axes of quantization of ions in a pair are oppositely aligned and, in consequence, their atomic tensors differ by a phase factor $(-1)^K$. These two features of the four pairs of ions are incorporated in the atomic tensors listed in Table I. Using the information in this table, for Eq. (3.1) one finds the result

$$\Psi_Q^{(K)}=\{1-(-1)^K\}\{e^{i\nu}[\langle T_Q^{(K)}(1)\rangle+(-1)^h e^{-i\varepsilon}\langle T_Q^{(K)}(7)\rangle] + e^{-i\nu}[\langle T_Q^{(K)}(5)\rangle+(-1)^h e^{i\varepsilon}\langle T_Q^{(K)}(3)\rangle]\}. \quad (3.3)$$

Evidently, the structure factor for charge-forbidden reflections ($h+k+l$ odd) is constructed from atomic tensors with $K=1$ and 3. The odd-rank tensors are purely magnetic and $\langle \mathbf{T}^{(1)}\rangle=\langle \mathbf{L}\rangle/\sqrt{30}$ and $\langle \mathbf{T}^{(3)}\rangle=\langle \Lambda\rangle/3\sqrt{70}$ where $\langle \mathbf{L}\rangle$ and $\langle \Lambda\rangle$ are, respectively, the orbital magnetic moment and the orbital octupole moment of the $3d$ valence shell of a resonant vanadium ion.

Vanadium ions at sites (1) and (5) are related by inversion. The atomic tensor, and $\mathbf{L}$, are unchanged by inversion and thus $\langle T_Q^{(K)}(1)\rangle=\langle T_Q^{(K)}(5)\rangle$. A similar relation holds for sites (3) and (7). Using this information in Eq. (3.3), and taking K to be an odd integer, one finds

$$\Psi_Q^{(K)}=4\{\cos(\nu)\langle T_Q^{(K)}(1)\rangle+(-1)^h\cos(\nu-\varepsilon)\langle T_Q^{(K)}(7)\rangle\}. \quad (3.4)$$

Ions at sites (1) and (7) are related by an a glide that includes reflection in the $\mathbf{a}_m-\mathbf{c}_m$ plane, which is normal to $\mathbf{a}_h=\mathbf{b}_m$. Reflection in the $\mathbf{a}_m-\mathbf{c}_m$ plane amounts to the change $x\rightarrow -x$, and with it $\langle T_Q^{(K)}\rangle\rightarrow(-1)^K\langle T_{-Q}^{(K)}\rangle$. For $K=1$ $(L_x,L_y,L_z)\rightarrow(L_x,-L_y,-L_z)$, so that reflection in the $\mathbf{a}_m-\mathbf{c}_m$ plane is accompanied by a change in the orientation of the orbital magnetization. The configuration of moments determined by Moon[3] is preserved if the polarity of the local field is now reversed, leading to $(L_x,-L_y,-L_z)\rightarrow(-L_x,L_y,L_z)$, for according to Moon $\langle L_x\rangle=0$ and the moments are confined to the $\mathbf{a}_m-\mathbf{c}_m$ plane. Reversing the polarity of the local field introduces in the atomic tensor a phase factor $(-1)^K$. The appropriate relation between tensors at sites (1) and (7) can be seen as a union of reflection in the $\mathbf{a}_m-\mathbf{c}_m$ plane and time reversal, and our discussion leads to the result $\langle T_Q^{(K)}(7)\rangle=\langle T_{-Q}^{(K)}(1)\rangle$; for simplicity of notation, we hereafter write $\langle T_Q^{(K)}\rangle=\langle T_Q^{(K)}(1)\rangle$.

In $\Psi_Q^{(K)}$ the phase angle ε is very small, and strong reflections are adequately described with $\varepsilon=0$. On using Eq. (3.4), our result for the atomic tensor for the vanadium ion at site (7), we arrive at

$$\Psi_Q^{(K)}=4\cos(\nu)\{\langle T_Q^{(K)}\rangle+(-1)^h\langle T_{-Q}^{(K)}\rangle\}. \quad (3.5)$$

Result (3.5) applies for $h+k+l$ odd (a charge-forbidden reflection) and K odd (purely magnetic diffraction), and it is the basis of the subsequent interpretation of azimuthal-angle scans performed on magnetically ordered V_2O_3. According to Eq. (3.5), reflections with h even are described by $\Psi_Q^{(K)}=\Psi_{-Q}^{(K)}$, whereas for h odd $\Psi_Q^{(K)}$ is an odd function of Q and $\Psi_0^{(K)}=0$.

In the monoclinic structure, sites occupied by the vanadium ions possess no spatial symmetry, and one can choose any set of axes for the associated atomic tensors. When proceeding from the corundum structure to the monoclinic one the average vanadium-oxygen distance remains essentially constant. This aspect of the structural transition, and others mentioned in Sec. II indicate that in the monoclinic structure the potential field experienced by a vanadium ion is principally referred to the trigonal axis, $\mathbf{c}_h$, and the field is almost subject to the requirement of a threefold axis of rotation. An atomic tensor invariant with respect to a threefold rotation is zero unless the projection index Q has the values 0 or ±3. Additions to the potential field, which reduce the symmetry from C_3 to one of no spatial symmetry, lift the restriction on the allowed values of Q.

At the first level of approximation, we can assume that the atomic tensor is diagonal with respect to principal axes in the monoclinic unit cell, and this means $\langle T_q^{(K)}\rangle_m=\delta_{q,0}\langle T_0^{(K)}\rangle_m$. The atomic tensor $\langle T_Q^{(K)}\rangle$, which arises in the structure factor calculated with Eq. (3.5) is defined with respect to orthogonal axes that contain $\mathbf{a}_h=\mathbf{b}_m$ and $\mathbf{c}_h$. Following findings from Moon,[3] the magnetic easy axis is taken to lie in the plane normal to $\mathbf{a}_h$ and cant at an angle ϕ with respect to $\mathbf{c}_h$. The relation between $\langle T_Q^{(K)}\rangle$ and $\langle T_q^{(K)}\rangle_m$ is then

$$\langle T_Q^{(K)}\rangle=\sum_q D_{qQ}^{(K)}\left(\frac{\pi}{2},\phi,-\frac{\pi}{2}\right)\langle T_q^{(K)}\rangle_m = D_{0Q}^{(K)}\left(\frac{\pi}{2},\phi,-\frac{\pi}{2}\right)\langle T_0^{(K)}\rangle_m, \quad (3.6)$$

where $D_{qQ}^{(K)}(\alpha,\beta,\gamma)$ is an element of the rotation matrix,[19] and the last equality follows if the atomic tensor $\langle T_q^{(K)}\rangle_m$ is diagonal.

Taking h even in Eq. (3.5), use of Eq. (3.6) leads to the result

$$\Psi_Q^{(K)}(h \text{ even})=8\cos(\nu)D_{0Q}^{(K)}(\pi/2,\phi,-\pi/2)\langle T_0^{(K)}\rangle_m. \quad (3.7)$$

Calculations of the intensity expected on the basis of Eq. (3.7) as the crystal is rotated about $\tau_m(hkl)$ are taken up in Sec. IV.

With h odd $\Psi_0^{(K)}=0$ and we are led to consider $\Psi_{\pm1}^{(1)}$, and $\Psi_Q^{(3)}$ evaluated for $Q=\pm1$, ±2, and ±3. Concerning $\Psi_{\pm1}^{(1)}$ we know that $\langle L_x\rangle=\langle L_{-1}-L_{+1}\rangle/\sqrt{2}=0$, because the magnetic moment is confined to the $\mathbf{a}_m-\mathbf{c}_m$ plane, and from this condition it follows that $\Psi_{\pm1}^{(1)}=0$. For diffraction enhanced by an $E1$ absorption event, which entails atomic tensors of rank up to $K=2$, we reach the conclusion that when both $h+k+l$ and h are odd the $E1$ structure factor is zero. This finding is consistent with the experimental observations.[8,9] Turning to the case of diffraction enhanced by an $E2$ event, we are left to consider

$$\Psi_Q^{(3)}(h \text{ odd})=4\cos(\nu)\{\langle T_Q^{(3)}\rangle-\langle T_{-Q}^{(3)}\rangle\} = \frac{4}{3\sqrt{70}}\cos(\nu)\sum_q D_{qQ}^{(3)}\left(\frac{\pi}{2},\phi,-\frac{\pi}{2}\right) \times\{\langle \Lambda_q\rangle_m-\langle \Lambda_{-q}\rangle_m\}. \quad (3.8)$$

IV. AZIMUTHAL-ANGLE SCANS

An azimuthal-angle scan is rotation of the crystal by an angle ψ about the Bragg wave vector τ_m (hkl). Looking along the $\mathbf{x}$ axis in Fig. 2 the rotation is in a clockwise direction. The origin $\psi=0$ is specified by a plane in recip-

rocal space normal to the plane of scattering. The plane in question is defined by τ_m and a second Bragg wave vector, which is either $(20\overline{2})_m$ or $(211)_m$. In orthogonal axes that include $\mathbf{a}_h$ and $\mathbf{c}_h$, $(20\overline{2})_m$ is parallel to $\mathbf{c}_h$ and $(211)_m$ is normal to $\mathbf{c}_h$.

A. *h* even

Experimental data are available for azimuthal-angle scans at $(2\overline{2}1)_m$, which is normal to $\mathbf{c}_h$. Writing $\tau_m/|\tau_m| = (t_1,t_2,t_3)$ for $(2\overline{2}1)_m$, one finds $t_1=-2/\sqrt{7}$, $t_2=(3/7)^{1/2}$ and $t_3=0$. [In the general case, t_1 and t_2 depend on (a/c) and $t_2/t_1=(h+l)/k\sqrt{3}$.] With $\psi=0$ the plane defined by τ_m and $(20\overline{2})_m$ is normal to the plane of scattering. Evidently, with $\psi=0$, the wave vector $(2\overline{2}1)_m$ can be aligned by rotation about $\mathbf{c}_h$ with the $\mathbf{x}$ axis in the experimental geometry, in which $\mathbf{H}^{(K)}$ is defined. The angle of rotation γ about $\mathbf{c}_h$ satisfies $\cos\gamma=-t_1$ and $\sin\gamma=t_2$, and result (3.7) transforms to

$$\Psi^{(K)}_{Q'}(h \text{ even}) = 8\cos(\nu) D^{(K)}_{0Q'}\left(\frac{\pi}{2},\phi,-\frac{\pi}{2}-\gamma\right)\langle T^{(K)}_0\rangle_m . \tag{4.1}$$

Rotation of the crystal by ψ about the $\mathbf{x}$ axis is described by the operation of $D^{(K)}_{Q'Q}(\pi/2,\psi,-\pi/2)$ on $\Psi^{(K)}_{Q'}$, and the diffracted amplitude in an azimuthal-angle scan is proportional to

$$\sum_{Q'} D^{(K)}_{Q'Q}\left(\frac{\pi}{2},\psi,-\frac{\pi}{2}\right)\Psi^{(K)}_{Q'}(h \text{ even}) = 8\cos(\nu) \times D^{(K)}_{0Q}\left(0,\beta_o,\gamma_o-\frac{\pi}{2}\right)\langle T^{(K)}_0\rangle_m . \tag{4.2}$$

In reaching this result we have used the addition theorem for components of the rotation matrix.[19] The angles β_o and γ_o are determined by

$$\cos\beta_o = \cos\phi\cos\psi - \sin\phi\sin\psi\cos\gamma$$

and

$$\cot\gamma_o = -\cos\psi\cot\gamma - \cot\phi\sin\psi/\sin\gamma. \tag{4.3}$$

As we shall see, these equations determine structure factors to within an overall phase factor that does not influence intensities.

The structure factor $F(\tau_m)$ is calculated from Eqs. (3.2) and (4.2), and one finds

$$F(\tau_m) = 8\cos(\nu)\sum_{K=1,3}(2K+1)^{1/2}\langle T^{(K)}_0\rangle_m \times \sum_Q (-1)^Q H^{(K)}_{-Q} D^{(K)}_{0Q}\left(0,\beta_o,\gamma_o-\frac{\pi}{2}\right). \tag{4.4}$$

In the experiments of interest the primary polarization is almost pure σ. Diffraction data have been collected in the unrotated $(\sigma'\sigma)$ and rotated $(\pi'\sigma)$ channels.

Using results for $H^{(K)}_Q$ listed in Ref. 18 the appropriate structure factors of immediate interest are

$$F_{\sigma'\sigma}(\boldsymbol{\tau}_m) = i\frac{2}{5}\cos(\nu)\sin 2\theta\cos\beta_o\langle L_0\rangle_m \times\left\{1+\frac{1}{3}\frac{\langle\Lambda_0\rangle_m}{\langle L_0\rangle_m}(3-5\cos^2\beta_0)\right\}, \tag{4.5}$$

and

$$F_{\pi'\sigma}(\tau_m) = i\frac{2}{5}\cos(\nu)\sin\beta_o\langle L_0\rangle_m\left\{\cos(3\theta-\gamma_o) + \frac{1}{12}\frac{\langle\Lambda_0\rangle_m}{\langle L_0\rangle_m}[3\cos(3\theta-\gamma_o)(5\cos^2\beta_o-1) - 5\cos(\theta-3\gamma_o)\sin^2\beta_o]\right\}. \tag{4.6}$$

As functions of ψ, fits of $|F(\tau_m)|^2$ to experimental data can provide values for the canting angle and the ratio of the diagonal components of the orbital octupole and magnetic moments. Note that $F_{\sigma'\sigma}(\tau_m)$ has a simple dependence on the Bragg angle, namely, $\sin 2\theta$, and with respect to ψ its magnitude is twofold periodic. In contrast, $F_{\pi'\sigma}(\tau_m)$ is not simple with respect to θ and ψ.

The diffraction patterns observed when neutrons are scattered by magnetically ordered V_2O_3 have been indexed with the reflections under discussion in this subsection, and it seems appropriate to consider the physical quantities that can be determined with this technique. In the limit of small Bragg angles, the amplitude for neutron diffraction is proportional to the magnetic moment and its principal component is $\mu_0=\langle L_0+2S_0\rangle_m$. Intensities are proportional to $\mu_0^2(1-k_\zeta^2)$, where k_ζ is the component of $\tau_m/|\tau_m|$ in the direction of the magnetic easy axis. Moon[3] observed 13 independent magnetic peaks of which $(010)_m$ is by far the strongest. This finding led Moon to propose that moments lie in the $\mathbf{a}_m-\mathbf{c}_m$ plane, which is normal to $(010)_m$, and one finds $k_\zeta=t_2\sin\phi+t_3\cos\phi$. By fitting intensities he found $\mu_0=1.2\pm0.1$ and $\phi=71°$.

In general, the amplitude for neutron diffraction depends on τ_m, and all the orbital moments of the $3d$ valence shell up to rank 4.[20] For example, the leading contribution made by the octupole moment is proportional to $(5k_\zeta^2-1)\langle\Lambda_0\rangle_m$, which might be distinguished from the other orbital moments by exploiting the dependence on the direction of τ_m.

B. *h* odd

Although the algebra in calculating $F(\tau_m)$ for h odd turns out to be more complicated than for h even, the steps involved are the same in both cases. First, $-\tau_m$ is aligned with the $\mathbf{x}$ axis. Values of the Euler angles α, β, and γ involved depend on the setting that defines the origin $\psi=0$. Secondly, the crystal is rotated by ψ about the $\mathbf{x}$ axis. For each of the two rotations there is an element of the rotation matrix, and in $F(\tau_m)$ the addition theorem reduces these to one component with Euler angles α_o, β_o, and γ_o.

The physical quantities that can be extracted, from fits of $|F(\tau_m)|^2$ to experimental data for intensities as a function of ψ, are components of the orbital octupole moment $\langle \Lambda_Q \rangle = \langle \Lambda_Q \rangle' + i\langle \Lambda_Q \rangle''$. More precisely, estimates of the following two ratios can be extracted:

$$r = (\tfrac{3}{5})^{1/2} \langle \Lambda_{+1} \rangle' / \langle \Lambda_{+3} \rangle' \tag{4.7}$$

and

$$t = \sqrt{6} \langle \Lambda_{+2} \rangle'' / \langle \Lambda_{+3} \rangle'. \tag{4.8}$$

In arriving at these results we have used the identity $\langle T^{(K)}_{-Q} \rangle = (-1)^Q \langle T^{(K)}_Q \rangle^*$.

The two structure factors of interest for analysing data with h odd are

$$F_{\sigma'\sigma}(\tau_m) = \frac{4i}{3\sqrt{5}} \langle \Lambda_{+3} \rangle' \cos(\nu) \sin 2\theta \sin \beta_o \Big\{ \sin^2 \beta_o \cos 3(\gamma - \alpha_o) + \frac{1}{2} t \sin 2\beta_o \sin 2(\gamma - \alpha_o) + r(5\cos^2 \beta_o - 1)\cos(\gamma - \alpha_o) \Big\}, \tag{4.9}$$

and

$$F_{\pi'\sigma}(\boldsymbol{\tau}_m) = -\frac{i}{3\sqrt{5}} \langle \Lambda_{+3} \rangle' \cos(\nu) \{ \sin 3(\gamma - \alpha_o)[4\cos A \sin B + \cos B \sin A(1 + 3\cos 2\beta_o)] + \cos 3(\gamma - \alpha_o)\cos \beta_o [4\cos A \cos B \cos^2 \beta_o + \sin A \sin B(\cos 2\beta_o - 5)] + 2t\{\sin 2(\gamma - \alpha_o)\sin \beta_o [\sin A \sin B \sin^2 \beta_o - 2\cos A \cos B \cos^2 \beta_o] + \cos 2(\gamma - \alpha_o)\sin 2\beta_o \cos B \sin A\} + r\{\sin(\gamma - \alpha_o)[4\cos A \sin B + \cos B \sin A(1 - 5\cos 2\beta_o)] + \cos(\gamma - \alpha_o)\cos \beta_o [4\cos A \cos B(4 - 5\cos^2 \beta_o) + \sin A \sin B(1 - 5\cos 2\beta_o)]\}). \tag{4.10}$$

Here $A = 2\gamma_o - 2\theta$ and $B = \gamma_o + \theta$. The intensity $|F_{\sigma'\sigma}|^2$ as a function of ψ is twofold periodic and, in general, $|F_{\pi'\sigma}|^2$ shows no such symmetry.

When the plane defined by τ_m and $(20\overline{2})_m$ is normal to the plane of scattering the Euler angles satisfy $t_1 = -\cos\beta\cos\gamma$, $t_2 = \cos\beta\sin\gamma$, $t_3 = -\sin\beta$, and $\alpha = 0$. Note that γ is independent of the cell dimensions. Upon rotation by ψ about the Bragg wave vector τ_m one needs to determine α_o, β_o, and γ_o from

$$\tan \alpha_o = -\frac{1}{\sin\beta} \tan\psi, \quad \cos\beta_o = \cos\beta\cos\psi,$$

$$\tan \gamma_o = -\tan\beta / \sin\psi. \tag{4.11}$$

Phases are fixed by conditions derived from the conservation with respect to ψ of the projection of a vector on the **x** axis, namely,

$$\sin\beta_o \sin\gamma_o = -\sin\beta \quad \text{and} \quad \sin\alpha_o \sin\beta_o = \sin\psi. \tag{4.12}$$

When the plane for the origin $\psi = 0$ is defined by τ_m and $(211)_m$ one finds $\alpha \neq 0$. In consequence, a determination of α, β, and γ entails considerable amounts of algebra and we refrain from giving details.

V. A CONFRONTATION OF EXPERIMENTAL DATA WITH CALCULATED INTENSITIES

Intensities $|F(\tau_m)|^2$ calculated as a function of the azimuthal angle from structure factors for h even, [Eqs. (4.5) and (4.6)] and h odd [Eqs. (4.9) and (4.10)] have been compared with data gathered at the Bragg wave vectors $\tau_m = (2\overline{2}1)_m$, $(111)_m$, and $(30\overline{2})_m$, for which the corresponding Bragg angles calculated with $\lambda = 2.27$ Å are $\theta = 36.9°$, 20.8°, and 34.2°. Best fits to the data collected at $(2\overline{2}1)_m$ and $(111)_m$ are displayed in Figs. 3 and 4. In this section we describe the fitting scheme and report values deduced for atomic quantities related to the orbital magnetism of V_2O_3 that afford a means of testing *ab initio* theories of the material.[7]

A confrontation between predictions of the theory and the data requires the input of several parameters. Some can be derived from geometrical considerations, such as Euler and Bragg angles, and are believed to be estimated fairly well; others are experimental in nature, particularly the zero setting for the azimuthal angle, but are thought to be calibrated reasonably well; some stem from material properties, e.g., r and t, and little is known about their values *a priori*. These varying degrees of uncertainty are easily taken into account within the Bayesian framework of data analysis[21] and, with suitable commonly used simplifying assumptions, lead to a somewhat generalized form of least-squares: in addition to a quadratic cost function for a mismatch with the measurements, there is also a penalty for deviating from those parameter values within the theory which are thought to be known fairly well. The best fits to data shown in Figs. 3 and 4, and at $(30\overline{2})_m$, utilize a robust simplex algorithm[22] for carrying out the (local) optimization.

Referring to Fig. 3, the quality of the fit is better for (π', σ) than (σ', σ), and this leads us to give greater credibility to the canting angle ϕ, deduced from $(\pi'\sigma)$ data. The intensity calculated for $(\sigma'\sigma)$ is twofold periodic in ψ; the

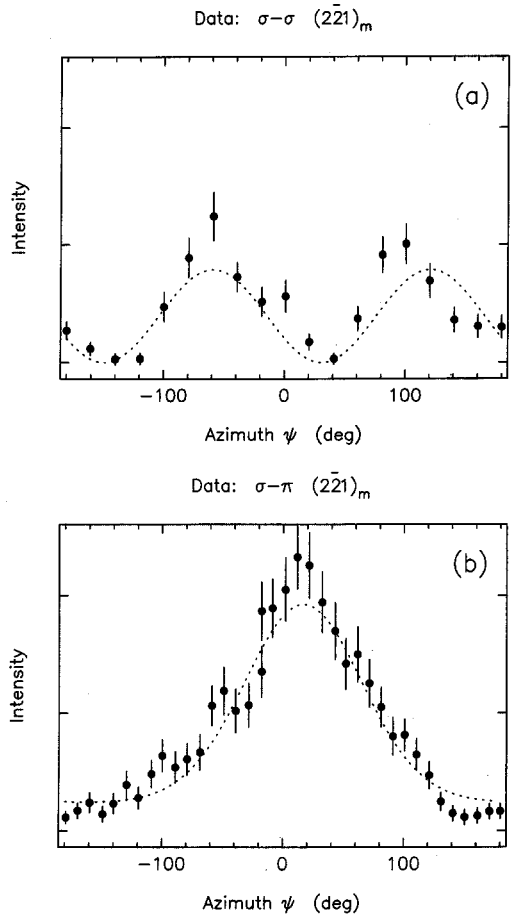

FIG. 3. Data gathered at the $(2\bar{2}1)_m$ reflection from V_2O_3, with 2.8% Cr doping, at 100 K (Ref. 9). The continuous curves are generated from expressions (4.5) and (4.6) with a Bragg angle $\theta = 36.9°$ ($\lambda = 2.27$ Å). From data gathered in the unrotated channel $(\sigma'\sigma)$ the fit gives $\phi = 66.1° \pm 2.1°$ and $\langle\Lambda_0\rangle_m/3\langle L_0\rangle_m = 0.00 \pm 0.05$; the corresponding values obtained from data in the rotated channel $(\pi'\sigma)$ are $\phi = 75.7° \pm 1.8°$ and $\langle\Lambda_0\rangle_m/3\langle L_0\rangle_m = -0.06 \pm 0.01$.

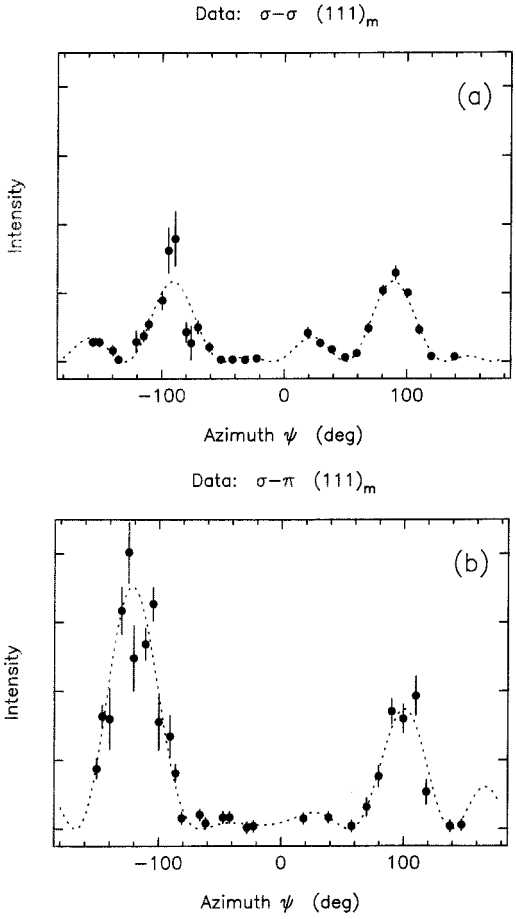

FIG. 4. Data on Cr-doped V_2O_3 held at a temperature of 0.55 $T_N = 100$ K and $\tau_m = (111)_m$, with $\theta = 20.8°$ (Ref. 8). From data in the unrotated channel and Eq. (4.9), we find $r = 0.33 \pm 0.04$ and $t = -0.35 \pm 0.15$, and from data in the rotated channel and Eq. (4.10) we find $r = 0.36 \pm 0.02$ and $t = -1.00 \pm 0.13$.

mismatch in the predicted and observed peak positions is not regarded as significant in the interpretation but attributed to ψ-dependent absorption.[10] Although the value of ϕ has not been constrained to be the same in Figs. 3(a) and 3(b), both sets of data are consistent with the angle which has been deduced by magnetic neutron diffraction.[3] While the $(\sigma'\sigma)$ data are not sensitive to $\langle\Lambda_0\rangle_m/3\langle L_0\rangle_m$, the $(\pi'\sigma)$ data indicate that this ratio is small and negative; using $\langle L_0\rangle_m \sim -0.5$,[8] one finds $\langle\Lambda_0\rangle_m \sim 0.09$.

Turning to h odd, we have analyzed data for $(111)_m$, which is displayed in Fig. 4, and data for $(30\bar{2})_m$.[8,10] The quality of the fits is better at $(30\bar{2})_m$ than at $(111)_m$. A signature of this feature of the data sets is that improved fits at $(111)_m$ are obtained on allowing some small lattitude in the Euler angles away from calculated values, namely $\alpha = 0$, $\beta = 12.7°$, and $\gamma = 130.9°$, while the quality of fits at $(30\bar{2})_m$ are barely improved on giving some lattitude to the Euler angles, which are calculated to be $\alpha = -7.0°$, $\beta = -78.4°$, and $\gamma = 121.4°$.

From data in the unrotated channel at $(30\bar{2})_m$ we find $r = 0.81 \pm 0.11$ and $t = 0.03 \pm 0.52$, and from corresponding data in the rotated channel $r = 1.24 \pm 0.24$ and $t = -0.19 \pm 0.13$. Evidently, data in the $(\sigma'\sigma)$ channel are not sensitive to t. Including the results for t obtained from data at $(111)_m$, it appears that $\langle\Lambda_{+2}\rangle''/\langle\Lambda_{+3}\rangle'$ is negative and of magnitude less than 1. Bringing together all the values for r we find $\langle\Lambda_{+1}\rangle'/\langle\Lambda_{+3}\rangle' \sim 0.9$.

VI. CONCLUSIONS

We have calculated structure factors for x-ray Bragg diffraction from magnetically ordered V_2O_3, with signal enhancement from the vanadium K-shell resonance, and successfully compared calculated intensities with data gathered in azimuthal-angle scans at space-group-forbidden reflections $(2\bar{2}1)_m$, $(111)_m$, and $(30\bar{2})_m$. As a function of the primary energy of the x rays the signal observed at 5.464 keV is fully consistent with a single-oscillator model. From this premise, the x-ray experiments in question reveal exclusively the orbital magnetization of V_2O_3, and quantities not directly obtainable with other experimental techniques.

Calculated structure factors conform to previously established chemical and magnetic structural properties, with no added elements of freedom. This approach respects evidence of a strong coupling of spin and orbital degrees of freedom in V_2O_3, seen in the relatively large orbital magnetic moment and pronounced magnetic anisotropy. At space-group forbidden reflections, the structure factors contain the following additional features.

(a) Reflections are purely magnetic, being associated with atomic moments of the vanadium $3d$-valence shell that are odd with respect to the reversal of time. In general, such moments vanish with the loss of long-range magnetic order. Our prediction for V_2O_3 is borne out in experiments which show that intensities decrease with increasing temperature, and vanish at the Néel temperature.

(b) A selection rule on the order of the electric absorption event and Miller indices h, k, and l. With $h+k+l$ odd (a space-group forbidden reflection) reflections with h odd do not contain a contribution from an $E1$ (electric dipole) event, and the finding is in accord with observations. In the reported calculation, the selection rule stems from the actual configuration of magnetic moments and the fact that they are contained in the $\mathbf{a}_m-\mathbf{c}_m$ plane.

(c) With h odd, diffraction is by anisotropic components of the orbital octupole moment of a vanadium ion. Such diffraction might be regarded as the magnetic equivalent of Templeton and Templeton scattering from a charge distribution.

(d) Intensities with h even can be used to determine the canting angle ϕ of the magnetic easy axis. Our analysis of data gathered at the pre-edge (5.464 keV) and $(2\bar{2}1)_m$ gives $\phi\sim 70°$ and the value is consistent with the analysis of intensities observed in magnetic neutron diffraction.[3] This outcome at the pre-edge, and related success in explaining other features, confirm that it is due mainly to an $E2$ resonance event.

(e) As a function of the azimuthal angle the calculated intensity in the channel with unrotated polarization $(\sigma'\sigma)$ is twofold periodic. This prediction and additional detail in calculated $(\sigma'\sigma)$ azimuthal angle scans is found in intensities collected at Bragg reflections $(2\bar{2}1)_m$, $(111)_m$, and $(30\bar{2})_m$.

(f) In general, the dependence on azimuthal-angle of intensities in the rotated channel $(\pi'\sigma)$ shows no systematic features. With h odd the $(\pi'\sigma)$ azimuthal angle scans have a quite complicated pattern, which essentially reflects the low symmetry (monoclinic) of the crystal below the Néel temperature.

(g) With regard to the nature of the ordering of orbital moments in the unit cell, relevant information is contained in our relation between atomic tensors for V ions at sites (1) and (7). Applied to the quadrupole moment $\langle\mathbf{Q}\rangle$, which transforms in the same way as the atomic tensor $\langle\mathbf{T}^{(2)}\rangle$, one finds that for the two sites in question, $\langle Q_{yz}\rangle$ and $\langle Q_{xx}-Q_{yy}\rangle$ have one sign while both $\langle Q_{xz}\rangle$ and $\langle Q_{xy}\rangle$ are of opposite sign at the two sites. All diagonal components of the quadrupole $\langle Q_{zz}\rangle$ are of one sign and independent of the site. [The orthogonal axes (x, y, z) are defined in Sec. III].

(h) The reflections referred to in (c) contribute in the neutron-diffraction pattern. Actual intensities are inferred by our findings in Sec. V. Calculated values are of the order of 10^{-3} relative to the $(010)_m$ contribution to the neutron-diffraction pattern.

ACKNOWLEDGMENTS

Dr. L. Paolasini has answered several enquiries about the execution of the experiments he and his colleagues have made on V_2O_3, and provided unpublished data to enhance our study. We are grateful to Professor E. Balcar, Dr. K. D. Finkelstein, Dr. S. Langridge, Dr. M. W. Long, and Dr. U. Staub for continued interest in our work on the interpretation of resonant x-ray Bragg diffraction. One of us (S.W.L.) has benefited from a discussion with Dr. R. M. Moon.

[1] D. B. McWhan, T. M. Rice, and J. P. Remeika, Phys. Rev. Lett. **23**, 1334 (1969).
[2] P. D. Dernier and M. Marezio, Phys. Rev. B **2**, 3771 (1970).
[3] R. M. Moon, Phys. Rev. Lett. **25**, 527 (1970).
[4] D. B. McWhan *et al.*, Phys. Rev. B **7**, 1920 (1973).
[5] N. F. Mott, *Metal-Insulator Transitions* (Taylor and Francis, London, 1990).
[6] M. Fabrizio, M. Altarelli, and M. Benfatto, Phys. Rev. Lett. **80**, 3400 (1998); F. Mila *et al.*, *ibid.* **85**, 1714 (2000).
[7] C. Castellani, C. R. Natoli, and J. Ranninger, Phys. Rev. B **18**, 4945 (1978); **18**, 4967 (1978); **18**, 5001 (1978); J.-H. Park *et al.*, *ibid.* **61**, 11 506 (2000); R. Shiina *et al.*, *ibid.* **63**, 144 422 (2001).
[8] L. Paolasini *et al.*, Phys. Rev. Lett. **82**, 4719 (1999).
[9] L. Paolasini *et al.*, J. Electron Spectrosc. Relat. Phenom. **120**, 1 (2001).
[10] L. Paolasini (private communication).
[11] S. W. Lovesey and K. S. Knight, J. Phys.: Condens. Matter **12**, L367 (2000).
[12] D. H. Templeton and L. K. Templeton, Phys. Rev. B **49**, 14 850 (1994).
[13] D. H. Templeton, Acta Crystallogr., Sect. A: Found. Crystallogr. **54**, 158 (1998).
[14] K. D. Finkelstein, Q. Shen, and S. Shastri, Phys. Rev. Lett. **69**, 1612 (1992).
[15] Y. Tanaka *et al.*, J. Phys.: Condens. Matter **11**, L505 (1999).
[16] S. W. Lovesey, J. Phys.: Condens. Matter **10**, 2505 (1998).
[17] W. Neubeck *et al.*, Phys. Rev. B **63**, 134430 (2001); J. Igarashi and M. Takahashi, Phys. Rev. B **63**, 184430 (2001).
[18] S. W. Lovesey, K. S. Knight, and E. Balcar, Phys. Rev. B **64**, 054405 (2001).
[19] D. A. Varshalovich, A. N. Moskalev and V. K. Khersonskii, *Quantum Theory of Angular Momentum* (World Scientific, Singapore, 1988).
[20] E. Balcar, S. W. Lovesey, and F. A. Wedgwood, J. Phys. C **6**, 3746 (1973).
[21] D. S. Sivia, *Data Analysis—A Bayesian Tutorial* (Oxford University Press, Oxford, 1996).
[22] J. A. Nelder and R. Mead, Comput. J. (Switzerland) **7**, 308 (1965).